Energy straggling of ^{4}He ions below 2.0 MeV in Al, Ni, Pt, and Au*

J. M. Harris and M.-A. Nicolet

California Institute of Technology, Pasadena, California 91125

(Received 19 August 1974; in final form 23 September 1974)

In recent years, backscattering spectrometry has become an important tool in the analysis of thin films. An inherent limitation, though, is the loss of depth resolution due to energy straggling of the beam. To investigate this, energy straggling of ^{4}He ions has been measured in thin films of Ni, Al, and Au. Straggling is roughly proportional to square root of thickness and appears to have a slight energy dependence. The results are compared with predictions of Bohr's theory and with previous measurements made in Pt. While Ni measurements are in fair agreement with theory, Al measurements are 30% above and Au measurements are 40% below predicted values. The Au and Pt measurements are consistent with one another.

INTRODUCTION

In recent years, ion beam backscattering spectrometry has been a remarkably successful microanalytical tool for investigating elemental composition, distribution, and lattice location. Backscattering has been extensively used to study problems occurring in the thin film and semiconductor industries.[1] Backscattering owes much of its success to the fact that it provides depth resolution. This depth resolution, though, is ultimately limited by the energy straggling of the incident beam as it penetrates the target. To estimate these limits, the energy straggling must be known.

He and H are the most common projectiles used for backscattering analysis in the energy range of 1–2 MeV. Experimental straggling data in solids are available for H,[2] but He data are rather scarce.[3] In the energy range below 2.0 MeV, He data for thin films are virtually nonexistent. Yet, this is just the region where backscattering spectrometry is typically used. Measurements of ^{4}He energy straggling below 2.0 MeV made in thin Al, Ni, and Au films are reported here along with previous measurements in Pt [4] including some unpublished ones at 1.5 and 1.7 MeV. These materials were selected as representative of light, medium, and heavy elements.

EXPERIMENTAL PROCEDURE

Energy straggling is the energy broadening due to the statistical nature of energy loss processes of the ion beam as it penetrates the target. The straggling is measured as the FWHM (full width at half maximum) of the energy profile of an initially monoenergetic beam which traverses a thin target. The incident beam is seldom monoenergetic and the detection system has a finite energy resolution. Both of these contribute to the FWHM of the transmitted beam energy profile and must be removed from it in order to obtain the energy straggling due to the target. The profile due to straggling for the effective target thickness and energy range's considered here has been measured and found closely approximated by a Gaussian.[4] The incident beam energy profile and the detection system response are also approximated by Gaussians, since they originate from random fluctuations in beam energy and the detection system. The energy profile of the transmitted beam, as measured, is a convolution of the incident beam profile, the detector response, and the energy straggling due to the target. Since all three distributions are Gaussians their FWHMs add quadratically

$$\Delta E_4^2 = \Delta E^2 + \Delta E^2_{\mathrm{DET}} + \Delta E^2_{\mathrm{BEAM}}, \tag{1}$$

where ΔE is the energy straggling due to the target, ΔE_4 is the measured FWHM of the transmitted ion beam energy profile, ΔE_{DET} is the FWHM of detector response function, and ΔE_{BEAM} is the FWHM of incident ion beam energy profile.

The effects of the incident beam profile and the detector are usually considered together and called the system resolution function. Using this in Eq. (1) and solving for the straggling yields,

$$\Delta E = (\Delta E_4^2 - \Delta E_1^2)^{\frac{1}{2}}, \tag{2a}$$

where

$$\Delta E_1 = \text{FWHM of the system resolution function} = (\Delta E^2_{\mathrm{DET}} + \Delta E^2_{\mathrm{BEAM}})^{\frac{1}{2}}. \tag{2b}$$

Traditionally, energy straggling was measured by transmitting a beam of particles through a self-supported thin film and directly determining ΔE_4.[3] This method relies on thin, highly uniform self-supported films which are difficult to produce and to handle. These problems are circumvented by measuring in a backscattering configuration, since the film can be deposited

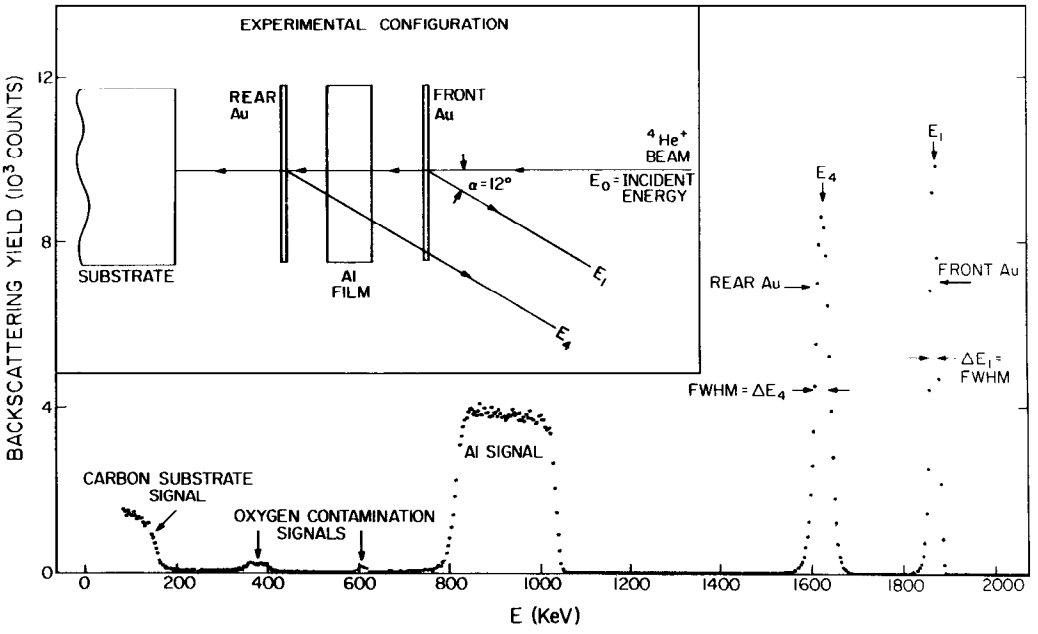

FIG. 1. 2.0 MeV, ^4He backscattering spectrum of an Al target with Au energy markers. Inset shows the experimental configuration.

on a rigid substrate. Furthermore, the quantities ΔE_1 and ΔE_4 can be obtained from a backscattering spectrum in several ways, depending on how the targets are prepared. However, when the backscattering configuration is used the beam must traverse the sample more than once and the elastic scattering event itself also affects the energy profile. So when comparing measurements with theory it must be remembered that the effective beam path length and the sample thickness are related by

$$\Delta R=\left(K+\frac{1}{\cos\alpha}\right)t, \tag{3}$$

where ΔR is the total ion path length, t is the sample thickness, K is the elastic scattering factor, and α is the scattering angle (see Fig. 1).

Complications are incurred when backscattering is used to make straggling measurements on light elements. The discontinuous energy loss due to the backscattering collision makes the incoming and outgoing particles lie in significantly different energy ranges. The energy dependence of the straggling then becomes somewhat complicated to unravel. This problem can be overcome by the use of energy markers.

Energy markers are made by depositing a very thin layer of a heavy metal, such as Pt or Au, before and after the film to be investigated is deposited (see inset Fig. 1). If the energy lost in traversing a marker is small compared to the system resolution, ΔE_1, then the system resolution function and the transmitted beam energy distribution will be displayed by the backscattering signals from the front and rear markers, respectively, without introducing significant perturbations. ΔE_1 and ΔE_4 can then be measured from these marker signals directly (see Fig. 1).

Such markers are particularly desirable for straggling measurements in films of low atomic number, as previously mentioned, because particles reflected by the heavy rear marker lose little energy in the scattering process. Thus, the energy of incoming and outgoing particles are in contiguous ranges, so that their energy loss and energy straggling are essentially those of particles traversing a film of thickness equal to the combined length of the incoming and outgoing tracks. The rear marker thus simulates a transmission experiment and circumvents any problems which might stem from the incoming and outgoing paths being in significantly different energy ranges [$K\cong 1$ in Eq. (3)].

To ascertain whether a marker is usable, the system resolution must be measured independently. ΔE_1 can be obtained from the high-energy edge of a backscattering spectrum taken on a thick target of an inert, heavy, monoisotopic element, such as Au. This edge is approximately the convolution of the system resolution function and the signal generated by the target's surface, which is assumed to be a step function. The high-energy edge thus represents the integral of the system resolution function. Since the system resolution function is assumed to be a Gaussian, ΔE_1 is the energy difference between the 12% and 88% points of the edge height.[4] Consequently, a marker is sufficiently thin if it indicates a system resolution which is indistinguishable from that measured on the high-energy edge of a clean Au target. All heavy markers used met this criterion and are typically 40-Å thick.

To determine the energy dependence of straggling, it is necessary to define an average energy over the particles' path. This, however, is easily done since in all the experiments reported here the incoming and outgoing particles lie in contiguous energy ranges. The average energy, $\bar{E}$, is the same used in calculating the beam energy loss, dE/dx, from a backscattering spectrum and is given by[5]

$$\bar{E}=\frac{E_1\cos\alpha+E_4}{1+K\cos\alpha}, \tag{4}$$

where E_0 is the mean energy of incident beam, E_1 is the mean energy of front marker signal $=KE_0$, E_4 is the mean energy of rear marker signal, and K is the elastic scattering factor for the marker material, ($K_{Pt}=0.922$, $K_{Au}=0.923$).

The average energy, defined in this way, reduces to the arithmetic average of E_0 and E_4 if $\alpha=0$ and $K=1$ (corresponding to an infinitely heavy marker). This is the average energy typically used in transmission experiments. The energy dependence of straggling is weak so the choice of how $\bar{E}$ is calculated is somewhat arbitrary since it has little influence on the results.

Markers offer no advantage for heavy elements and are not used. If markers are not present E_1, E_4, ΔE_1, and ΔE_4 are obtained from the backscattering signal of the bulk film. The front and rear edges of this signal represent the integrals of the system resolution function and the transmitted beam energy profile, respectively. Thus, E_1 and E_4 are the 50% height points of the front and rear edges, respectively. Furthermore, ΔE_1 and ΔE_4 are the energy differences between the 12% and 88% points of the front and rear edges (see Ref. 4 for more details).

EXPERIMENTAL PROCEDURE

A. Sample Preparation

Depositions were all made by evaporation onto clean polished substrates. Evaporations were performed using an electron gun in an oil free vacuum system at pressures lower than 1×10^{-6} Torr. Dummy samples on vacuum baked, polished carbon substrates were prepared simultaneously with the targets and used to check for light contaminants, such as oyxgen, in the films. Film thicknesses were measured using a multiple-beam interferometer.

Ni samples were prepared by first depositing a Pt marker on a Si substrate, then annealing at 280°C for about $\frac{1}{2}$ h in a dry N_2 atmosphere. The Pt reacts with the substrate forming PtSi.[6] This prevents the marker from mixing with Ni during the Ni evaporation. The Ni film and top marker were deposited sequentially without breaking vacuum.

Al samples were prepared by sequentially depositing onto Si or SiO_2 substrates an Au marker, an Al film and a top Au marker without breaking vacuum. Precautions against mixing were not necessary, probably because small amounts of Al_2O_3 form in the initial stages of evaporation, creating a diffusion barrier between Au and Al.

Au targets were prepared by evaporation of Au onto Si substrates.

B. Sample and Apparatus Evaluation

Since high-quality samples are critical to straggling measurements, the samples were examined for defects which might lead to erroneous straggling results. Among the sample properties investigated were contamination level, lateral uniformity, surface roughness, and temperature stability.

Contamination was checked by backscattering spectrometry on the dummy samples and oxygen was found to be the chief contaminant. Other contaminants were either lighter than C or present in concentrations too small to be detected (see Fig. 1). By far the highest oxygen contamination was found in the Al samples (typically 2 at.%). Contamination by oxygen at these concentrations should not influence the straggling measurements in any significant way.

To ascertain lateral uniformity, backscattering spectra taken from different parts of the sample were compared. The samples were found to be uniform (variations $<2\%$).

The surface roughness was investigated using a scanning electron microscope. The surface of the sample appeared featureless. Any surface irregularities present were beyond the resolution of the microscope used ($\sim$400 Å). Surface roughness was not investigated farther because previous investigations using a tally step (resolution $\sim$100 Å) on Cr samples prepared similarly revealed that samples made on polished Si substrates were smooth to the order of that instrument's resolution.

The temperature stability of the films was investigated by annealing a completed target in a dry N_2 atmosphere for $\frac{1}{2}$ h at 200°C. No change in the backscattering signal was noted.

Experiments were made to investigate the possible influence of carbon deposition on the target during irradiation and of irradiation on the measurements. Spectra taken at various beam currents, for various lengths of time and with various beam sizes were compared with one another. No significant differences were observed and the straggling evaluated from these spectra were all consistent with one another.

The stability and linearity of the backscattering apparatus were checked by taking a backscattering spectrum of various elements ranging from C to Pt with the beam at a given energy, E_0. The front edge energy, F_1, of each element can be calculated

$$E_1=K_{\text{element}}E_0. \tag{5}$$

If the beam energy is stable and the energy detection system is linear and stable, a plot of the calculated energy E_1 vs the channel number corresponding to the frong edge 50% height points should yield a straight line. The apparatus was found to be sufficiently linear and stable (deviations $<0.5\%$ for irradiation times in excess of 18 h) to perform the straggling measurements. These last tests were performed *in situ* during straggling measurements made on each set of samples.

To check for systematic errors in the measurements, dE/dx was calculated from the backscattering spectra[5] and compared with current values in the literature.[7] No significant deviations were observed. (For discussion of dE/dx measurements using markers see Ref. 8.)

TABLE I. Results of measurements taken in Al, Ni, Pt, and Au.

t(A°)	E_0 (MeV)	E_1 (MeV)	E_4 (MeV)	$\bar{E}$ (MeV)	ΔE_1 (keV)	ΔE_4 (keV)	ΔE (keV)
Al	$\rho=2.7$ g/cc		$N=6.0\times10^{22}$ atoms/cc		Au markers used		
1221	2.0	1.846	1.778	1.883	18.84	22.77	12.8
2188	2.0	1.846	1.726	1.856	20.34	27.12	17.9
3584	2.0	1.846	1.649	1.815	18.84	29.19	22.3
4681	2.0	1.846	1.577	1.778	19.44	33.22	26.9
1221	1.5	1.385	1.313	1.411	18.48	23.35	14.2
2188	1.5	1.385	1.253	1.370	19.10	26.57	18.5
3584	1.5	1.385	1.165	1.324	18.49	29.06	22.4
4681	1.5	1.385	1.084	1.282	19.90	33.29	26.7
1221	1.0	0.923	0.841	0.916	17.87	22.74	14.1
2188	1.0	0.923	0.773	0.881	16.87	25.74	16.5
3584	1.0	0.923	0.677	0.830	18.44	28.6	21.8
Ni	$\rho=8.9$ g/cc		$N=9.13\times10^{22}$ atoms/cc		Pt markers used		
1274	2.0	1.844	1.688	1.835	21.60	28.32	18.3
3730	2.0	1.844	1.381	1.674	19.92	37.92	32.3
5151	2.0	1.844	1.213	1.585	20.16	42.96	37.9
1274	1.5	1.383	1.219	1.352	18.72	26.00	18.0
2426	1.5	1.383	1.062	1.269	18.32	29.94	23.7
3730	1.5	1.383	0.900	1.184	18.12	32.51	26.9
5151	1.5	1.383	0.743	1.102	18.52	38.81	34.1
2426	1.0	0.922	0.59	0.784	16.44	27.74	22.3
3730	1.0	0.922	0.443	0.707	16.87	31.17	26.2
Pt[b]	$\rho=21.4$ g/cc		$N=6.6\times10^{22}$ atoms/cc				
4554	2.0	1.844	1.232	1.596	16.8	39.2	35.4
3747	2.0	1.844	1.333	1.650	16.8	35.0	30.5
3333	2.0	1.844	1.396	1.708	16.8	33.6	29.2
2532	2.0	1.844	1.494	1.734	16.8	30.8	25.9
2532	2.0	1.844	1.504	1.739	15.0	32.2	27.5
2532[a]	2.0	1.878	1.504	1.737	4.0	27.0	26.8
2005	2.0	1.844	1.579	1.779	15.0	27.4	25.1
1482	2.0	1.844	1.650	1.816	15.0	26.6	21.7
1482[a]	2.0	1.873	1.662	1.822	4.0	21.0	20.6
1170	2.0	1.844	1.689	1.837	15.0	23.8	18.2
1170[a]	2.0	1.870	1.709	1.847	4.0	18.0	17.6
483[a]	2.0	1.873	1.807	1.904	4.5	12.0	11.3
202[a]	2.0	1.876	1.847	1.926	6.0	10.0	8.0
4554	1.7	1.57	0.939	1.30	18.3	37.9	33.4
3333	1.7	1.57	1.112	1.39	18.2	33.1	27.7
2567	1.7	1.57	1.215	1.45	18.2	29.8	23.6
1482	1.7	1.57	1.362	1.52	17.1	26.8	20.6
1169	1.7	1.57	1.402	1.55	17.9	25.2	17.7
4554	1.5	1.38	0.745	1.11	18.1	35.6	30.7
3333	1.5	1.38	0.918	1.19	17.5	31.5	26.2
2567	1.5	1.38	1.022	1.25	17.6	29.4	23.5
2532[a]	1.5	1.406	1.014	1.24	4.0	18.0	26.1
1482	1.5	1.38	1.67	1.32	16.6	26.2	20.2
1170	1.5	1.38	1.211	1.35	16.1	23.5	17.0
1170[a]	1.5	1.407	1.222	1.354	6.0	18.0	17.0
4554	1.0	0.922	0.288	0.626	15.8	37.4	34.0
3747	1.0	0.922	0.380	0.674	15.8	36.0	32.4
3333	1.0	0.922	0.437	0.704	15.8	32.0	27.5
2532	1.0	0.922	0.534	0.755	15.8	27.3	22.3
2005	1.0	0.922	0.617	0.799	15.2	25.9	21.0
1482	1.0	0.922	0.695	0.839	14.4	23.0	18.0
1170	1.0	0.922	0.739	0.863	14.4	20.1	14.4
1170[a]	1.0	0.935	0.740	0.860	4.0	13.5	12.5
202[a]	1.0	0.933	0.902	0.949	4.0	6.2	5.8
Au	$\rho=19.3$ g/cc		$N=5.9\times10^{22}$ atoms/cc				
6114	2.0	1.846	0.923	1.43	22.82	50.85	45.4
2407	2.0	1.846	1.526	1.75	21.02	33.67	26.3
1712	2.0	1.846	1.621	1.80	19.21	30.06	22.5
860	2.0	1.846	1.737	1.87	18.78	25.31	17.0
6114	1.5	1.385	0.505	0.978	22.51	49.77	44.4
2407	1.5	1.385	1.037	1.26	18.71	30.93	25.6
1712	1.5	1.385	1.143	1.30	26.59	33.88	21.0
860	1.5	1.385	1.266	1.38	18.12	22.66	13.6
2407	1.0	0.923	0.577	0.778	16.87	28.46	22.9
1712	1.0	0.923	0.676	0.830	16.87	26.03	19.8
860	1.0	0.923	0.801	0.895	16.87	21.59	13.5

[a] Measurements were taken with solid state detector at backscattering angle of 168° ($\alpha=12°$, see Fig. 1), except for those marked with an asterisk (*) which were taken with magnetic analyzer at a backscattering angle of 150°. Energy markers were used for measurements in Al and Ni only.

[b] Additional measurements at 1.5 and 1.7 MeV are included with the data of Harris and Chu (Ref. 4).

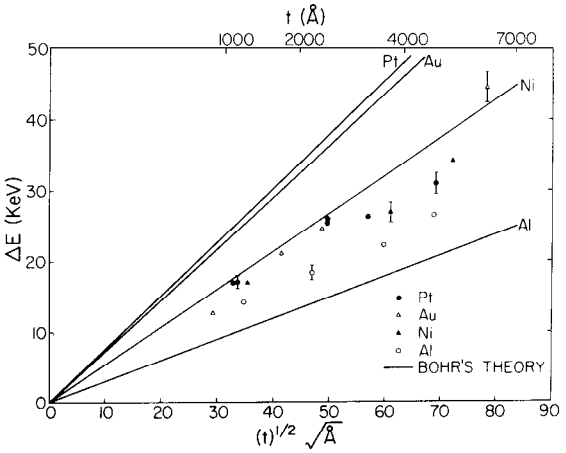

FIG. 2. ^{4}He energy straggling for an incident energy of 1.5 MeV vs square root root of target thickness. In addition to measurements made in Al, Ni, and Au, predictions of Bohr's theory and some previous measurements made in Pt[4] are given.

RESULTS

The results of measurements in Al, Ni, and Au along with the Pt data taken previously[4] are contained in Table I. Table I also contains some additional 1.5 and 1.7-MeV Pt measurements which were not published previously. Results using 1.5-MeV incident beam are typical, and are presented in Fig. 2 along with the Pt data and Bohr's Theory,[9] according to which,

$$\Delta E^2=4\pi(2.355)^2e^4Z_1^2(NZ_2\Delta R), \qquad (6)$$

where e is the electronic charge; Z_1, atomic number of incident particles; Z_2, atomic number of target; ΔR, effective path length [see Eq. (3)]; and N is the atomic density.

Straggling is proportional to the square root of target thicknesses for the elements, thicknesses and energy ranges covered, as predicted by Bohr's theory. However, the theory tends to overestimate straggling in all the elements shown except Al, where measurements are about 15% higher than predictions. The straggling measurements in both Pt and Au give nearly the same values. These are about 30% below the theory. The Ni measurements are in closest agreement with the theory which overestimates them by only about 10%. As one can see in Fig. 2 there is a systematic increase in straggling with increase in atomic number; however, it is not as strong a function as Bohr's theory indicates.

To display the energy dependence it is convenient to divide the straggling by $(NtZ_2)^{\frac{1}{2}}$. This normalization reduces Bohr's theory to a universal curve. All the results and the Pt data are thus normalized and plotted vs the average energy in Fig. 3. One can see that the energy dependence of straggling is at most weak. Straggling seems to decrease with decrease in energy, however, uncertainties in the experimental values are such that a more precise characterization is difficult. Straggling in Ni seems to show a somewhat stronger energy dependence than straggling in the remaining elements.

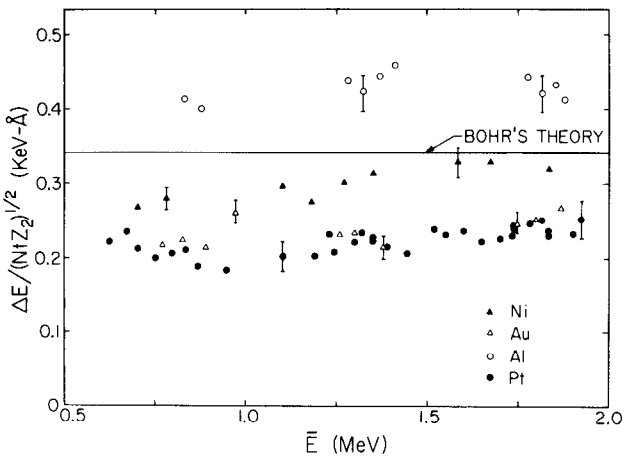

FIG. 3. Normalized ^{4}He energy straggling vs average energy for Al, Ni, Pt, and Au.[4]

The main statistical error in these measurements originates from the energy differences ΔE_1 and ΔE_4, which cannot be determined to better than ± 1 channel corresponding to about ± 2.0 keV. This error, when added in quadrature with smaller statistical errors and propagated, yields an estimated uncertainty of about 10% in ΔE. Representative error bars are given for ΔE in Figs. 2 and 3. Error bars for the thickness are omitted in this figure since the resulting uncertainty in the abscissa ($\sim$2.5%) is typically the size of the symbol used.

DISCUSSION AND CONCLUSION

Energy straggling of ^{4}He ions in Al, Ni, Pt, and Au is proportional to the square root of target thickness, increases with target atomic number, and has a weak energy dependence. For the most part these characteristics are adequately described by Bohr's theory. However, predictions of Bohr's theory overestimate straggling by about 30% in Au and Pt and underestimates it by about 15% in Al. Straggling in Ni is closest to theory.

Since Bohr's theory is so easy to calculate and describes the general characteristics of straggling well it is sufficient for most applications where a rough estimate is necessary. However, a number of other theories exist.[10,11] These theories employ various levels of sophistication to deal with atomic structure, which makes some of them rather difficult to evaluate. For that reason, and since Bohr's theory is adequate for most applications, other theories are not discussed here.

From the data in Table I one can determine the ultimate depth resolution obtainable for various thicknesses of Al, Ni, Pt, and Au. For example, given a detection system of 20 keV, straggling is the resolution-limiting process at 1.5 MeV for Ni targets, which are over about 2000-Å thick.

*Work supported by O.N.R. (L. Cooper).

[1]W. K. Chu, J. W. Mayer, M.-A. Nicolet, T. M. Buck, G. Amsel, and F. Eisen, Thin Solid Films **17**, 1 (1973).
[2]C. B. Madsen and P. Venkateswarlu, Phys. Rev. **74**, 1782 (1948); C. B. Madsen, Dan. Mat. Fys. Medd. **27**, 13 (1953); L. P. Nielsen, Dan. Mat. Fys. Medd. **33**, 6 (1961).
[3]J. R. Comfort, J. E. Decker, E. T. Lynk, M. O. Scully, and A. R. Quniton, Phys. Rev. **150**, 249 (1966); F. Denichelis, Nuovo Cimento **13**, 2134 (1959); D. A. Sykes and S. J. Harris, Nucl. Instrum. Methods **94**, 39 (1971).
[4]J. M. Harris, W. K. Chu, and M.-A. Nicolet, Thin Solid Films **19**, 259 (1973).
[5]R. D. Moorhead, J. Appl. Phys. **36**, 391 (1965); W. D. Warters, Ph.D. dissertation, Caltech, 1953.
[6]A. Hiraki, M.-A. Nicolet, and J. W. Mayer, Appl. Phys. Lett. **18**, 178 (1971).
[7]J. F. Ziegler and W. K. Chu, IBM Res. Report. RC4288 (#19193). Also Thin Solid Films **19**, 281 (1973); J. A. Borders, Rad. Eff. **16**, 253 (1972).
[8]W. White, R. M. Mueller, Phys. Rev. **187**, 449 (1969); D. A. Thompson and W. D. Macintosh, J. Appl. Phys. **42**, 3969 (1971).
[9]N. Bohr, Dan. Mat. Fys. Medd. **18**, 8 (1948).
[10]J. Lindhard, Kgl Danske Videnskab Selskab, Mat.-Fys. Medd. **28**, 8 (1954); J. Lindhard and A. Winther, Kgl. Danske Videnskab Selskab, Mat.-Fys. Medd. **34**, 4 (1964); C. Tschalar, Nucl. Instrum. Methods **61**, 141 (1968); 237 (1968), U. Fano, Ann. Rev. Nucl. Sci. **13**, (1963).
[11]J. Harris and M.-A. Nicolet, Phys. Rev. (to be published).